

# Resonance width distribution for high-dimensional random media

Matthias Weiss<sup>1</sup>, J. A. Méndez-Bermúdez<sup>2,3</sup>, and Tsampikos Kottos<sup>2,4</sup>

<sup>1</sup>*Cellular Biophysics Group (BIOMS), German Cancer Research Center,  
Im Neuenheimer Feld 580, D-69121 Heidelberg, Germany*

<sup>2</sup>*Max-Planck-Institut für Dynamik und Selbstorganisation, Bunsenstrasse 10, D-37073 Göttingen, Germany*

<sup>3</sup>*Department of Physics, Ben-Gurion University, Beer-Sheva 84105, Israel and*

<sup>4</sup>*Department of Physics, Wesleyan University, Middletown, CT 06459-0155, USA*

(Dated: August 15, 2018)

We study the distribution of resonance widths  $\mathcal{P}(\Gamma)$  for three-dimensional (3D) random scattering media and analyze how it changes as a function of the randomness strength. We are able to identify in  $\mathcal{P}(\Gamma)$  the system-inherent fingerprints of the metallic, localized, and critical regimes. Based on the properties of resonance widths, we also suggest a new criterion for determining and analyzing the metal-insulator transition. Our theoretical predictions are verified numerically for the prototypical 3D tight-binding Anderson model.

PACS numbers: 03.65.Nk, 71.30.+h, 72.20.Dp, 73.23.-b

## I. INTRODUCTION

Quantum mechanical scattering in systems with complex internal dynamics has been a subject of intensive research activity for a number of years. The interest was motivated by various areas of physics, ranging from nuclear<sup>1</sup>, atomic<sup>2</sup> and molecular<sup>3</sup> physics, to mesoscopics<sup>4</sup>, quantum chaos<sup>5,6</sup>, and classical wave scattering<sup>7</sup>. Recently, the interest in this subject was renewed due to technological developments in quantum optics associated with the construction of new type of lasers<sup>8,9</sup> and the experimental investigation of atoms in optical lattices<sup>10</sup>.

The most fundamental object which characterizes the process of quantum scattering is the scattering matrix  $S$ , where  $S$  relates the amplitudes of waves that enter and leave a scattering region. Of great interest are the statistical properties of the poles of the  $S$  matrix. They determine the conductance fluctuations of a quantum dot in the Coulomb blockade regime<sup>11</sup> or the current relaxation<sup>12</sup>. The poles of the  $S$  matrix are related to resonance states occurring at complex energies  $\mathcal{E}_n = E_n - \frac{i}{2}\Gamma_n$ , where  $E_n$  is the position and  $\Gamma_n$  the width of the resonance. Resonances correspond to “eigenstates” of the open system that decay in time due to the coupling to the “outside world”.

For chaotic systems Random Matrix Theory (RMT) is applicable and the distributions of resonance widths  $\mathcal{P}(\Gamma)$  is known. A review can be found in Ref. 13 (see also Ref. 14). As the disorder increases, the system becomes diffusive and the deviations from RMT increase drastically. For low dimensional random systems in the metallic regime the distribution of resonances  $\mathcal{P}(\Gamma)$  was found recently<sup>15,16,17</sup>. For the strongly disordered limit, where localization dominates,  $\mathcal{P}(\Gamma)$  was investigated by various groups<sup>18,19,20</sup> as well. At the same time an attempt to understand systems at critical conditions was undertaken in Refs. 21 and 22. The latter deals with random systems of higher dimensions, the most prominent of which is the three-dimensional (3D) Anderson

model. It undergoes a Metal-Insulator Transition (MIT) with increasing strength of disorder<sup>23</sup>.

In this paper we extend our previous analysis on the 3D Anderson model<sup>22</sup> and study the distribution of resonance widths as we change the disorder strength. Based on the analysis of  $\mathcal{P}(\Gamma)$  we propose a new method to locate the MIT. The paper is organized as follows: In Section II the 3D Anderson model and the scattering formalism are introduced. In Sec. III we discuss the consequences of localization in the distribution of resonance widths in the diffusive and localized regimes as well as at the MIT and show the numerical results supporting our arguments. In Sec. IV we investigate a new method for determining and analyzing the emergence of the MIT and propose a scaling theory near the critical point. Finally, our conclusions are given in Sec. V.

## II. THE 3D ANDERSON MODEL AND THE SCATTERING SETUP

The Anderson model with diagonal disorder on a 3D cubic lattice is described by the tight-binding Hamiltonian (TBH)

$$H_0 = \sum_{\mathbf{n}} | \mathbf{n} \rangle W_{\mathbf{n}} \langle \mathbf{n} | + \sum_{(\mathbf{n}, \mathbf{m})} | \mathbf{n} \rangle \langle \mathbf{m} |, \quad (1)$$

where  $\mathbf{n} \equiv (n_x, n_y, n_z)$  labels all the  $N = L^3$  sites of the cubic lattice, while the second sum is taken over all nearest-neighbor pairs  $(\mathbf{n}, \mathbf{m})$  on the lattice. The on-site potential  $W_{\mathbf{n}}$  for  $1 \leq n_x, n_y, n_z \leq L$  is independently and identically distributed with probability  $\mathcal{P}(W_{\mathbf{n}})$ . We use three different distributions for the random potential: (a) a box distribution, i.e., the  $W_{\mathbf{n}}$  are uniformly distributed on the interval  $[-W/2, W/2]$ ; (b) a Gaussian distribution with zero mean and variance  $W^2/12$ ; and (c) a Cauchy distribution  $\mathcal{P}(W_{\mathbf{n}}) = W/\pi(W_{\mathbf{n}}^2 + W^2)$ . For the system defined by Eq. (1) the MIT for  $E \simeq 0$  occurs for  $W = W_c$  with (a)  $W_c \simeq 16.5$ , (b)  $W_c \simeq 21.3$ , and (c)  $W_c \simeq 4.26$

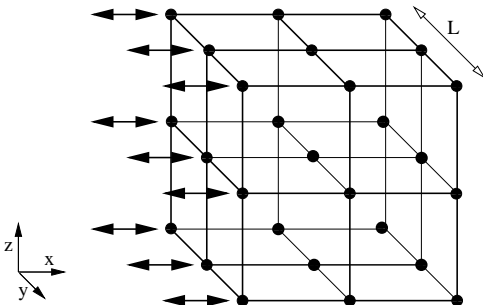


FIG. 1: Scattering setup. The sample is a cubic lattice of linear length  $L$ . To each of the  $M = L^2$  sites of the layer  $n_x = 1$  semi-infinite single mode leads are attached.

(see Ref. 24). Then, for  $W < W_c$  ( $W > W_c$ ) the system is in the metallic (insulating) regime.

We turn the isolated system to a scattering one by attaching  $M = L^2$  semi-infinite single mode leads to each site of the layer  $n_x = 1$ , as depicted in Fig. 1. Each lead is described by a one-dimensional semi-infinite TBH

$$H_M = \sum_{n=1}^{-\infty} (|n\rangle\langle n+1| + |n+1\rangle\langle n|). \quad (2)$$

Using standard methods<sup>1</sup> one can write the scattering matrix in the form<sup>21,22</sup>

$$S(E) = \mathbf{1} - 2i \sin(k) \mathcal{W}^T (E - \mathcal{H}_{\text{eff}})^{-1} \mathcal{W}, \quad (3)$$

where  $\mathbf{1}$  is the  $M \times M$  unit matrix,  $k = \arccos(E/2)$  is the wave vector supported in the leads, and  $\mathcal{H}_{\text{eff}}$  is an effective non-hermitian Hamiltonian given by

$$\mathcal{H}_{\text{eff}} = H_0 - e^{ik} \mathcal{W} \mathcal{W}^T. \quad (4)$$

Here,  $\mathcal{W}$  is a  $N \times M$  matrix that specifies at which site of the sample we attach the leads. Its elements are equal to zero or  $\sqrt{w}$ , with  $0 < \sqrt{w} \leq 1$ , where  $w$  is the coupling strength. Below, unless stated otherwise, we will always consider the case  $w = 1$ . Moreover, since  $\arccos(E/2)$  changes only slightly in the center of the band, we set  $E = 0$  and neglect the energy dependence of  $\mathcal{H}_{\text{eff}}$ . The poles of the  $S$  matrix are then equal to the complex zeros of

$$\det[\mathcal{E} - H_{\text{eff}}] = 0. \quad (5)$$

From Eqs. (3) and (5) it is clear that the formation of resonances is closely related to the dynamics in the scattering region, governed by  $H_0$ .

In order to investigate the distributions of resonance widths we used samples with  $L = 20$  as a maximum size. For better statistics a considerable number of different disorder realizations was considered. In all cases we had at least 10 000 data for statistical processing.

### III. DISTRIBUTION OF RESONANCE WIDTHS: RESULTS AND DISCUSSION

#### A. Metallic Regime

When the disorder strength  $W$  is smaller than  $W_c$ , but still large enough so that the mean free path is smaller than the system size, the system is in the metallic regime.

Recently, a lot of research activity was devoted to the understanding of the statistical properties of various physical quantities (such as conductance, local density of states, current relaxation times) in finite-size random systems in the metallic regime. The outcome of these studies indicated that the tails of these distribution functions show large deviations from the universal Random Matrix Theory (RMT) results, expected to be valid<sup>25</sup> in the limit of infinite dimensionless conductance  $g = \Gamma_{\text{Th}}/\Delta = DL$ . Here,  $\Gamma_{\text{Th}} \sim D/L^2$  is the typical inverse time (Thouless time) that an excitation needs to diffuse (with diffusion coefficient  $D$ ) in order to reach the boundary of a system, with linear size  $L$ , and  $\Delta \sim 1/L^3$  is the mean level spacing.

The origin of these deviations was found to be related to the existence of eigenstates which are unusually localized around a center of localization. These states are precursors of the Anderson localization and were termed *prelocalized* states<sup>26,27,28,29</sup>. In 3D conductors they have sharp amplitude peaks on the top of a homogeneous background<sup>26,27</sup>.

We start our analysis by investigating the effects of prelocalized states in the distribution of resonance widths. It is natural to expect that these states with localization centers at the bulk of the sample are affected only weakly when opening the system at the boundaries. Therefore, prelocalized states decay very slowly to the continuum leading us to the conclusion that the corresponding resonance widths (inverse lifetime)  $\Gamma$  are smaller than the mean level spacing  $\Delta$ . Hence, assuming the validity of standard first order perturbation theory (that can be applied if the coupling of the sample to the leads is weak,  $w \ll 1$ ) we get

$$\frac{\Gamma}{2} = \langle \Psi | \mathcal{W}^\dagger \mathcal{W} | \Psi \rangle \propto \sum_{n \in \text{boundary}} |\Psi(n)|^2 \sim L^2 |\Psi(L)|^2, \quad (6)$$

where  $|\Psi(L)|^2$  is the wavefunction intensity of a prelocalized state at the boundary of the sample. At the same time, the distribution of wavefunction components at the boundary was found to be<sup>27</sup>

$$\mathcal{P}(\theta) \sim \exp[-C_1 \ln^3(\theta)], \quad (7)$$

with  $\theta^{-1} = L\Psi(L)$  and  $C_1 \propto g$ . Using Eq. (7) together with Eq. (6) we obtain

$$\mathcal{P}(1/\Gamma) \sim \exp[-C_2 \ln^3(1/\Gamma)], \quad (8)$$

where  $C_2 \propto g$ .

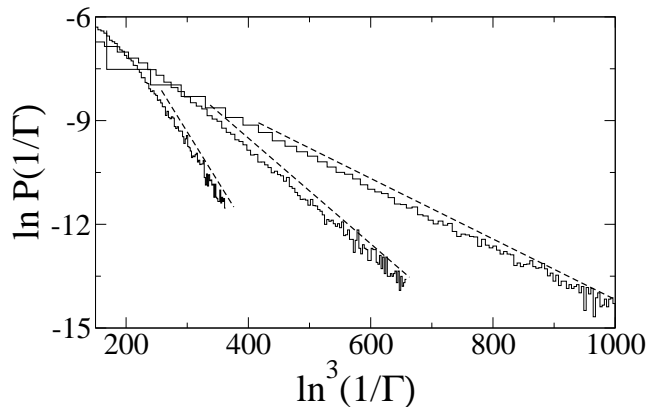


FIG. 2: The distribution of resonance widths, plotted as  $\mathcal{P}(1/\Gamma)$  vs  $\ln^3(1/\Gamma)$ , for  $\Gamma < \Delta$  in the diffusive regime.  $L = 16$  and  $W = 10, 12$ , and  $14$  (from left to right). The dashed lines are (shifted) linear fittings to the distributions.

As can be seen from Fig. 2 the prediction of Eq. (8), obtained using perturbation theory, holds even for strong coupling. Indeed, the reported data for the 3D Anderson model in the diffusive regime, plotted as  $\ln \mathcal{P}(1/\Gamma)$  vs  $\ln^3(1/\Gamma)$ , shows a linear behaviour. This comes as a surprise since in Fig. 2 we have considered perfect coupling,  $w = 1$ . Differences in slope correspond to different dimensionless conductances  $g$  induced by the varying values of disorder strengths.

Next, we turn to the analysis of  $\mathcal{P}(\Gamma)$  for  $\Gamma \gtrsim \Gamma_{\text{Th}} \gg \Delta$ . In order to go on we need to recall that the inverse of  $\Gamma$  represents the quantum lifetime of a particle in a resonant state escaping into the leads. Moreover, we assume that the particles are uniformly distributed inside the sample and spread until they reach the boundary where they are absorbed. Then, we can associate the corresponding lifetimes with the time  $t_R \sim 1/\Gamma_R$  a particle needs to reach the boundaries, when starting a distance  $R$  away. The relative number of states that require a time  $t < t_R$  in order to reach the boundaries (or equivalently the number of states with  $\Gamma > \Gamma_R$ ) is

$$\mathcal{P}_{\text{int}}(\Gamma_R) = \int_{\Gamma_R}^{\infty} \mathcal{P}(\Gamma) d\Gamma \sim \frac{V(t_R)}{L^3}, \quad (9)$$

where  $V(t_R) \sim L^3 - (L - R)^3$  is the volume populated by all particles with lifetimes  $t < t_R$ .

Assuming now diffusive spreading,

$$R^2 = D \cdot t_R,$$

we get from Eq. (9) (to leading order with respect to  $\Gamma_{\text{Th}}/\Gamma$ )

$$\mathcal{P}(\tilde{\Gamma}) \sim \left( \frac{\tilde{\Gamma}_{\text{Th}}}{\tilde{\Gamma}} \right)^{3/2} = \left( \frac{g}{\tilde{\Gamma}} \right)^{3/2} \quad (10)$$

where we refer to the rescaled variable  $\tilde{\Gamma} = \Gamma/\Delta$ . Equation (10) is valid as long as the leads are attached to the

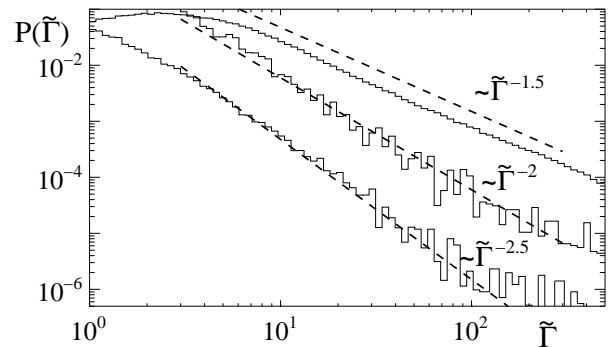


FIG. 3: The resonance width distribution  $\mathcal{P}(\tilde{\Gamma})$  for  $L = 16$  and various scattering configurations (from up to down):  $M = L^2$  leads attached to the boundary, one lead attached to the boundary, and one lead attached to a site in the bulk of the sample. The dashed lines are the corresponding theoretical predictions for  $\Gamma \gtrsim \Gamma_{\text{Th}}$  given by Eqs. (10-12), see main text.

boundary of the sample.

Here, it is interesting to point out that a different way of opening the system might lead to a different power law behavior for  $\mathcal{P}(\Gamma)$ . Such a situation can be realized if instead of opening the system at the boundaries we attach one lead somewhere in the sample. In such a case we have

$$\mathcal{P}_{\text{int}}(\Gamma_R) \sim \frac{V(t_R)}{L^3} \approx \frac{R^3}{L^3} = \frac{(D \cdot t_R)^{3/2}}{L^3} \sim \left( \frac{\Gamma_{\text{Th}}}{\Gamma_R} \right)^{3/2},$$

leading to

$$\mathcal{P}(\Gamma) \sim \Gamma^{-5/2}, \quad (11)$$

where we used  $V(t_R) \sim R^3$ . The above results are correct for any number of leads  $M$  such that the ratio  $M/L^3$  scales as  $1/L^3$ .

If, on the other hand, we attach a single lead to the boundary of the sample we obtain

$$\mathcal{P}(\Gamma) \sim \Gamma^{-2}. \quad (12)$$

This behavior is due to the fact that the decay takes place at the surface, leading to a situation similar to that of a 2D system<sup>17</sup>.

In Fig. 3 we present numerical data for the 3D Anderson model in the metallic regime. We verify the validity of the theoretical predictions given by Eqs. (10-12) by using various configurations:  $M = L^2$  leads attached to the boundary, one lead attached to the boundary, and one lead attached to a site in the bulk of the sample, respectively. We observe a good agreement with the expected behavior in all cases.

## B. Localized Regime

When the disorder strength  $W$  is larger than  $W_c$  the system is in the localized regime. In this regime the eigen-

functions are exponentially localized in space and, as a consequence, transmission is inhibited and the system behaves as an insulator.

Various groups<sup>18,19,20</sup> had investigated the resonance width distribution of low dimensional random media in the localized regime during the last years. In the region of exponentially narrow resonances  $\Gamma < \Gamma_0 = \exp(-2L/l_\infty)$  the distribution was found to be log-normal, i.e.,

$$\mathcal{P}(\tilde{\Gamma}) \sim \exp \left[ - \left( 4 \frac{L}{l_\infty} \right)^{-1} \ln^2(\tilde{\Gamma}) \right], \quad \Gamma < \Gamma_0. \quad (13)$$

This result is analogous to the conductance distribution of localized systems. Equation (13) essentially relies on two assumptions: first, that eigenfunction components are randomly distributed with no long-range correlations; and second, that they are exponentially localized with a normal distribution of localization lengths.

It is reasonable to assume that the same arguments leading to Eq. (13) applies as well for high-dimensional random media like the 3D Anderson model in the localized regime. Indeed, our numerical results reported in Fig. 4(a) show good agreement with the theoretical expectation (13) which supports our assumption.

On the other hand, we found [see Fig. 4(b)] that the long tails of the distribution behave as

$$\mathcal{P}(\tilde{\Gamma}) \sim \left( \frac{l_\infty}{L} \right) \frac{1}{\tilde{\Gamma}}, \quad \Gamma_0 < \Gamma \ll 1/L. \quad (14)$$

Equation (14) can be easily understood when employing Eq. (9). The new ingredient is that wavefunctions are exponentially localized:  $|\Psi(r)| \sim l_\infty^{-3/2} \exp(-r/l_\infty)$ . Using simple perturbation arguments<sup>18</sup> [see Eq. (6)], i.e.  $\Gamma \sim |\Psi(r)|^2$ , we obtain

$$R^3 \sim l_\infty^3 \ln^3(l_\infty^3 \Gamma).$$

By inserting this into Eq. (9) we get Eq. (14), to leading order with respect to  $l_\infty/L$ .

The region of large  $\Gamma$  values is essentially determined by the coupling to the continuum, so it should be model-dependent. Nevertheless, it is reasonable to assume that the number of resonances involved is constant, of order  $l_\infty$ , and therefore the extreme tail of the distribution should subside at large  $L$  at the rate  $\sim l_\infty/L$ .

Let us finally note that in the thermodynamic limit  $L \rightarrow \infty$  the probability of finding an eigenstate at any finite distance from the boundary is equal to zero. Thus the distribution of the resonance widths in this case approaches a delta function centered at zero.

### C. Criticality

The MIT, where  $W = W_c$ , is characterized by several *critical* properties: the level statistics acquires a scale-independent form<sup>26,30,31,32</sup> while the eigenfunctions show

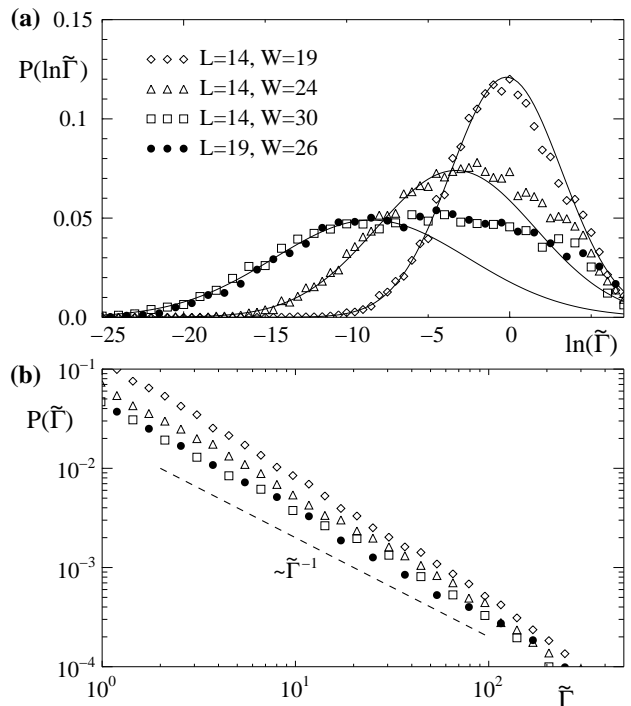


FIG. 4:  $\mathcal{P}(\tilde{\Gamma})$  in the localized regime for various combinations of  $W$  and  $L$  in the range  $\tilde{\Gamma} \leq 1$ . The log-normal decay is highlighted by Gaussian fits (full curves) whose maximum decreases with increasing strength of disorder and also shifts towards smaller values of  $\tilde{\Gamma}$ . When keeping the ratio  $l_\infty/L \approx 0.136$  fixed, similar distributions were obtained for different combinations of  $L$  and  $W$  (filled circles and open squares). (b) For  $\tilde{\Gamma} \geq 1$  the power-law decay  $\mathcal{P}(\tilde{\Gamma}) \sim 1/\tilde{\Gamma}$  is observed (dashed line) which becomes more robust for increasing strength of disorder.

strong fluctuations on all length scales and obey multifractal distributions<sup>26,27,33,34,35</sup>.

In Ref. 22 it was found that  $\mathcal{P}(\tilde{\Gamma})$  follows a new universal distribution, i.e., independent of the microscopic details of the random potential and number of attached leads. Specifically, it decays asymptotically with the power

$$\mathcal{P}(\tilde{\Gamma}) \sim g_c^{1/3} \tilde{\Gamma}^{-(1+1/3)}, \quad (15)$$

which is different from those found for chaotic, metallic, or localized systems (see Ref. 13, Eq. (10), and Eq. (14), respectively).

One can relate the power-law decay (15) to the anomalous diffusion at the MIT. Indeed, at the MIT the conductance of a 3D disordered sample has a finite value  $g_c \sim 1$ . Approaching the MIT from the metallic regime one has  $g \sim E_T/\Delta$ , where  $E_T = D/R^2$  is the Thouless energy,  $D$  is the diffusion coefficient, and  $\Delta \sim 1/R^3$  is the mean level spacing of a sample with linear size  $R$ . This yields  $D \sim g_c/R$  at  $W_c$ . Taking into account that  $D = R^2/t_R$ , we get for the spreading of an excitation at

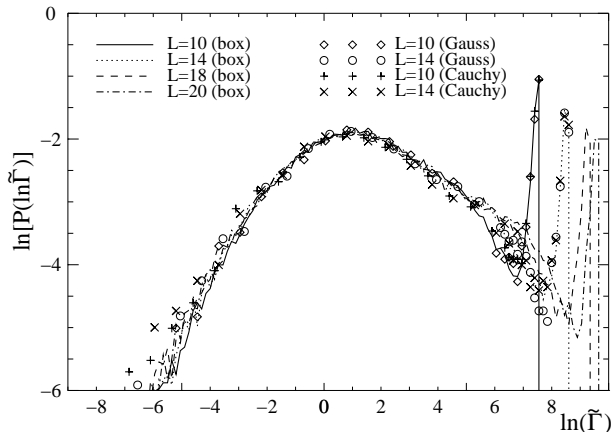


FIG. 5: Universal behavior of  $\mathcal{P}(\tilde{\Gamma})$  at the MIT [reported here as  $\mathcal{P}(\ln(\tilde{\Gamma}))$ ] for various sample sizes  $L$  and potential distributions.

the MIT

$$R^3 \sim g_c \cdot t_R .$$

Then, straightforward application of Eq. (9) leads to Eq. (15).

In Figs. 5 and 6 we report some numerical results for the 3D Anderson model at the MIT. Figure 5 shows the distribution of the logarithm of the rescaled resonance widths  $\mathcal{P}(\ln(\tilde{\Gamma}))$  for the three different distributions  $\mathcal{P}(W_n)$  of the random potential and for various sample sizes  $L$ . The body of the distribution function in all cases coincides and does not change its shape or width. Of course, the far tail of this universal distribution develops better with increasing  $L$ . The sharp peak appearing at the right is an artifact of our choice to neglect the energy dependence of  $\mathcal{H}_{\text{eff}}$ . We thus confirm that at the MIT the distribution of rescaled resonances is indeed scale-invariant independent of the microscopic details of the potential.

From Fig. 6(a) an inverse power law  $\mathcal{P}_{\text{int}}(\tilde{\Gamma}) \sim \tilde{\Gamma}^{-\alpha}$  is evident. The best fit to the numerical data yields  $\alpha = 0.333 \pm 0.005$  in accordance with Eq. (15). Here, the case of perfect coupling ( $w = 1$ ) has been considered. Different coupling strengths are going to affect this behavior as can be seen from Fig. 6(b).

#### IV. A SCALING THEORY FOR THE RESONANCES WIDTHS

In the original proposal of the scaling theory of localization, the conductance  $g$  is the relevant parameter<sup>23,36</sup>. A manifestation of this statement is seen in Eqs. (8,10,13,14,15) where  $\mathcal{P}_{\text{int}}^0 \equiv \mathcal{P}_{\text{int}}(\tilde{\Gamma}_0)$  is proportional to the conductance  $g$ . It is therefore natural to expect that  $\mathcal{P}_{\text{int}}^0$  will follow a scaling behavior for finite  $L$

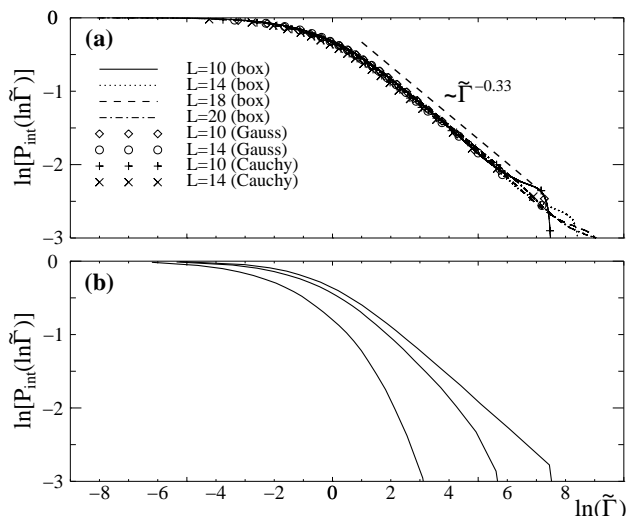


FIG. 6: (a) The integrated distribution  $\mathcal{P}_{\text{int}}(\tilde{\Gamma})$  in the case of perfect coupling,  $w = 1$ , for various sample sizes  $L$  and potential distributions. The dashed line is the theoretical prediction  $\mathcal{P}_{\text{int}}(\tilde{\Gamma}) \sim \tilde{\Gamma}^{-0.333}$ , see Eq. (15). (b)  $\mathcal{P}_{\text{int}}(\tilde{\Gamma})$  for a box distribution,  $L = 10$ , and different coupling strengths:  $w = 0.001$ ,  $0.01$ , and  $0.5$  from left to right.

(and for some  $\tilde{\Gamma}_0 \sim 1$ ) that is similar to the one obeyed by the conductance  $g$ . The following scaling hypothesis was therefore postulated in Ref. 22:

$$\mathcal{P}_{\text{int}}^0(W, L) = f(L/l_\infty(W)) . \quad (16)$$

In the insulating phase ( $W > W_c$ ) the conductance of a sample with length  $L$  behaves as  $g(L) \sim \exp(-L/l_\infty)$  due to the exponential localization of the eigenstates, and therefore we have  $g(L_1) < g(L_2)$  for  $L_1 > L_2$ . Based on Eq. (15) we expect the same behavior for  $\mathcal{P}_{\text{int}}^0$ ; i.e., for every finite  $L_1 > L_2$  we must have  $\mathcal{P}_{\text{int}}^0(W, L_1) < \mathcal{P}_{\text{int}}^0(W, L_2)$ . On the other hand, in the metallic regime ( $W < W_c$ ) we have that  $g(L) = DL$  and therefore we expect from Eq. (15)  $\mathcal{P}_{\text{int}}^0(W, L_1) > \mathcal{P}_{\text{int}}^0(W, L_2)$ . Thus, the critical point is the one at which the size effect changes its sign, or in other words, the point where all curves  $\mathcal{P}_{\text{int}}^0(W, L)$  for various  $L$  cross. One can reformulate the last statement by saying that in the thermodynamic limit  $L \rightarrow \infty$  at  $W = W_c$  the number of resonances with width larger than the mean level spacing goes to a constant.

In Fig. 7, we show the evolution of  $\mathcal{P}_{\text{int}}^0(W)$  for different values of  $L$  using the box distribution. From this analysis the critical disorder strength  $W = W_c = 16.5 \pm 0.5$  was determined in agreement with other calculations<sup>24</sup>. A further verification of the scaling hypothesis (16) is shown in Fig. 8 where the same data are reported as a function of the scaling ratio  $L/l_\infty$ . Note that all points collapse on two separate branches for  $W < W_c$  and  $W > W_c$ .

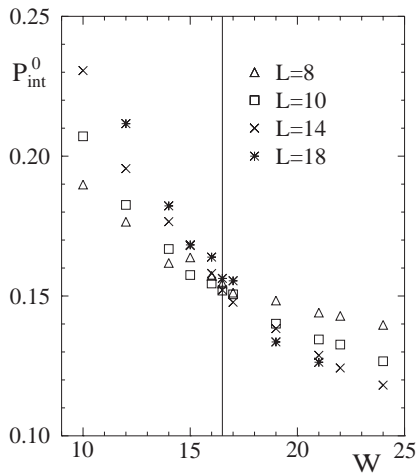


FIG. 7:  $\mathcal{P}_{\text{int}}^0(W, L)$  as a function of  $W$  for different system sizes  $L$  provides a means to determine the critical point  $W_c$  of the MIT (vertical line at  $W = 16.5$ ).

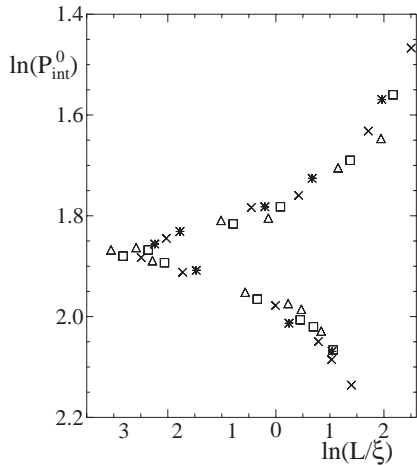


FIG. 8: The one-parameter scaling of  $\mathcal{P}_{\text{int}}^0(W, L)$  [Eq. (16)] is confirmed for various system sizes  $L$  and disorder strengths  $W$  using the box distribution.

## V. CONCLUSIONS

We have studied the properties of the resonance width distribution in various regimes for the 3D Anderson model.

In the metallic regime we obtained the forms of  $\mathcal{P}(\Gamma)$  for small and large  $\Gamma$  and show that they are determined by the underlying diffusive dynamics and by the existence of prelocalized states. For the localized regime we also explored the limits of small and large  $\Gamma$ . In the first limit we found that  $\mathcal{P}(\Gamma)$  shows a log-normal behavior while in the latter the distribution is power-law like. At the MIT we show that  $\mathcal{P}(\tilde{\Gamma})$ , with  $\tilde{\Gamma} = \Gamma/\Delta$ , has a *universal* form, i.e., independent of the microscopic details of the random potential and number of attached leads. Specifically, it decays asymptotically with a power which is different from those found in the diffusive and localized regimes. In addition, based on resonance widths, we suggested a new method for determining and analyzing the emergence of the MIT and propose a scaling theory near the critical point.

## VI. ACKNOWLEDGMENTS

T. K. acknowledges many useful comments and discussions with Prof. B. Shapiro. J.A.M.-B. and T.K. acknowledge support by a grant from the GIF, the German-Israeli Foundation for Scientific Research and Development. M.W. acknowledges support from the BIOMS initiative in Heidelberg.

<sup>1</sup> C. Mahaux and H. A. Weidenmüller, *Shell Model Approach in Nuclear Reactions*, (North-Holland, Amsterdam), (1969); I. Rotter, Rep. Prog. Phys. **54**, 635 (1991); J. J. M. Verbaarschot, H. A. Weidenmüller, M. R. Zirnbauer, Phys. Rep. **129**, 367 (1985).  
<sup>2</sup> M. H. Nayfeh et al., *Atomic Spectra and Collisions in External Fields*, eds. (Plenum, New York), Vol. 2 (1989).  
<sup>3</sup> P. Gaspard, in *Quantum Chaos, Proceedings of E. Fermi Summer School 1991*, G. Casati et al., eds. (North-Holland) 307.  
<sup>4</sup> C. Beenakker, Rev. Mod. Phys. **69**, 731 (1997).  
<sup>5</sup> U. Smilansky, in *Les Houches Summer School on Chaos and Quantum Physics*, M.-J. Giannoni et al., eds. (North-Holland) 371-441 (1989).

<sup>6</sup> H.-J. Stöckmann *Quantum Chaos: An Introduction*, Cambridge Univ. Press (1999); E. Kogan, P. A. Mello, H. Liqun, Phys. Rev. E **61**, R17 (2000); C.W.J. Beenakker and P.W. Brouwer, Physica E **9**, 463 (2001).  
<sup>7</sup> E. Doron, U. Smilansky, A. Frenkel, Phys. Rev. Lett. **65**, 3072 (1990); H. J. Stöckmann, J. Stein, Phys. Rev. Lett. **64**, 2215 (1990); J. Stein, H.-J. Stöckmann, and U. Stöckmann, Phys. Rev. Lett. **75**, 53 (1995).  
<sup>8</sup> D. S Wiersma, M. P. Van Albada, A. Lagendijk, Nature (London) **373**, 203 (1995); A. Z. Genack et al. Phys. Rev. Lett. **82**, 715 (1999).  
<sup>9</sup> J. U. Nockel and A. D. Stone, Nature (London) **385**, 45 (1997); C. Gmachl et al., Science **280**, 1556 (1998).  
<sup>10</sup> M. Raizen, C. Salomon, Q. Niu, Physics Today **50** 30-34

- (1997).
- <sup>11</sup> I. L. Aleiner, P. W. Brouwer, L. I. Glazman, Phys. Rep. **358**, 309 (2002); Y. Alhassid, Rev.Mod.Phys. **72**, 895 (2000).
  - <sup>12</sup> B. L. Altshuler, V. E. Kravtsov, I. V. Lerner, in *Mesoscopic Phenomena in Solids*, eds. B. L. Altshuler, P. A. Lee and R. A. Webb (North Holland, Amsterdam), (1991).
  - <sup>13</sup> Y. V. Fyodorov, H-J Sommers, J. Math. Phys. **38** 1918 (1997).
  - <sup>14</sup> T. Kottos and U. Smilansky, Phys. Rev. Lett. **85**, 968 (2000); Journal of Physics A: Math. and General **36**, 3501 (2003).
  - <sup>15</sup> F. Borgonovi, I. Guarneri, D. Shepelyansky, Phys. Rev. A **43**, 4517 (1991).
  - <sup>16</sup> A. Ossipov, Tsampikos Kottos and T. Geisel, Phys. Rev E **65**, 055209(R) (2002).
  - <sup>17</sup> A. Ossipov, Tsampikos Kottos and T. Geisel, Europhys. Lett. **62**, 719 (2003).
  - <sup>18</sup> M. Titov and Y. V. Fyodorov, Phys. Rev. B **61**, R2444 (2000); M. Terraneo, and I. Guarneri, Eur. Phys. J. B **18**, 303 (2000).
  - <sup>19</sup> Starykh OA, Jacquod PRJ, Narimanov EE, Stone AD, Phys. Rev. E **62**, 2078 (2000).
  - <sup>20</sup> F. A. Pinheiro, M. Rusek, A. Orłowski, B. A. van Tiggelen, Phys. Rev. E **69**, 026605 (2004).
  - <sup>21</sup> F. Steinbach, A. Ossipov, Tsampikos Kottos, and Theo Geisel, Phys. Rev. Lett., **85** 4426, (2000).
  - <sup>22</sup> T. Kottos and M. Weiss, Phys. Rev. Lett., **89** 056401, (2002).
  - <sup>23</sup> P. W. Anderson, Phys. Rev. **109**, 1492 (1958); A. MacKinnon and B. Kramer, Rep. Prog. Phys. **56**, 1469 (1993)
  - <sup>24</sup> A. Cohen, Y. Roth and B. Shapiro, Phys. Rev. B **38**, 12125 (1988); C. M. Soukoulis, X. S. Wang, Q. M. Li, M. M. Sigalas, Phys. Rev. Lett. **82**, 668 (1999); K. Slevin and T. Ohtsuki, *ibid.* **82**, 382 (1999); K. A. Muttalib and P. Wölffe, *ibid.* **83**, 3013 (1999); P. Markos, *ibid.* **83**, 588 (1999).
  - <sup>25</sup> K. B. Efetov, Adv. Phys. **32**, 53 (1983); K. B. Efetov, *Supersymmetry in Disorder and Chaos*, (Cambridge University Press, Cambridge, 1997).
  - <sup>26</sup> A. D. Mirlin, Phys. Rep. **326**, 259 (2000).
  - <sup>27</sup> V. I. Fal'ko and K. B. Efetov, Europhys. Lett. **32**, 627 (1995); Phys. Rev. B **52**, 17413 (1995); B. A. Muzykantskii and D. E. Khmel'nitskii, Phys. Rev. B **51**, 5480 (1995); Y. V. Fyodorov and A. Mirlin, Int. J. Mod. Phys. B **8**, 3795 (1994); I. Smolyarenko and B. L. Altshuler, Phys. Rev. B **55**, 10451 (1997).
  - <sup>28</sup> Tsampikos Kottos, A. Ossipov and T. Geisel, Phys. Rev E **68**, 066215 (2003).
  - <sup>29</sup> V. Uski, B. Mehl'ig, R. A. Römer, and M. Schreiber, Phys. Rev. B **62**, R7699 (2000); V. Uski, B. Mehl'ig, and M. Schreiber, *ibid.* **63**, 241101(R) (2001); B. Nikolić, Phys. Rev. B **64**, 014203 (2001).
  - <sup>30</sup> B. I. Shklovskii, B. Shapiro, B. R. Sears, P. Lambrianides, and H. B. Shore, Phys. Rev. B **47**, 11487 (1993)
  - <sup>31</sup> B. L. Alt'shuler and B. I. Shklovskii, Zh. Eksp. Teor. Fiz. **91**, 220 (1986) [Sov. Phys. JETP **64**, 127 (1986)]; A. G. Aronov, A. D. Mirlin, Phys. Rev. B **51**, 6131 (1995); V. E. Kravtsov and I. V. Lerner, Phys. Rev. Lett. **74**, 2563 (1995); I. Zharekeshev and B. Kramer, Jpn. J. Appl. Phys. **34**, 4361 (1995).
  - <sup>32</sup> J. T. Chalker, V. E. Kravtsov and I. V. Lerner, Pis'ma Zh. Eksp. Teor. Fiz. **64**, 355 (1996) [JETP Lett. **64**, 386 (1996)].
  - <sup>33</sup> F. Wegner, Z. Phys. B **36**, 209 (1980).
  - <sup>34</sup> M. Schreiber and H. Grussbach, Phys. Rev. Lett. **67**, 607 (1991); D. A. Parshin and H. R. Schober, *ibid.* **83**, 4590 (1999); A. Mildenberger, F. Evers, and A. D. Mirlin, Phys. Rev. B **66**, 033109 (2002).
  - <sup>35</sup> F. Evers and A. D. Mirlin, Phys. Rev. Lett. **84**, 3690 (2000); E. Cuevas, M. Ortuno, V. Gasparian, and A. Perez-Garrido, *ibid.* **88**, 016401 (2002); I. Varga, Phys. Rev. B **66**, 094201 (2002); I. Varga and D. Braun, *ibid.* **61**, R11859 (2000).
  - <sup>36</sup> E. Abrahams, P. W. Anderson, D. C. Licciardello, and T. V. Ramakrishnan, Phys. Rev. Lett. **42**, 673 (1979); L. P. Gorkov, A. I. Larkin and D. E. Khmel'nitskii, JETP Lett. **30** 228 (1979).